

Characterizing Geometrical Anisotropy of Petrophysical properties in the middle Shahejie formation, Liaohe Depression, China.

***Oluwatosin J. Rotimi^{1,2}, Zhenli Wang² and Richard O. Afolabi¹**

¹*Petroleum Engineering Department, Covenant University, Ota, Nigeria.*

²*Key Laboratory of Petroleum Resources, Institute of Geology and Geophysics, CAS, Beijing, China.*

Abstract

Knowledge of reservoir body lateral extent is important information for estimation of hydrocarbon initially in place and the recoverable quantity. This study reports a stepwise approach to evaluate geometrical anisotropy of the rapidly changing alluvial fan Shahejie formation of Eocene age. This is towards understanding reservoir geometry of the deposit beneath the flank of Bohai bay, Northern China. Computation of Sand net to gross (Volume of shale), porosity and permeability was done on well logs as an initial analytical step, followed by computation of sample variograms, data transformation and property modeling. Computation of semivariance was based on first geometrical anisotropy for autocorrelation by finding major and minor directions of data consistency. Autocorrelation of data with distance of location made upscaled data useful for stochastic simulation.

Minor data direction is almost perpendicular to the major direction with the bandwidth of not less than 4000. In the vertical direction, average bandwidth is 50. Porosity for the modeled zone is consistent with values between 17% and 35%. Permeability is consistent briefly away from well location but higher in shale units. These oil impregnated shale units are laterally consistent in the up-dip portion but were overtaken by the clastic units in the distal portion. This made draining of hydrocarbon better done in the down-dip portion of the area. An excellent comparative analysis was made of the lithofacies model, petrophysical properties, and inversion results obtained from the vintage seismic. This has yielded a good result in characterizing variation in rock properties of the subtle laterally inconsistent synsedimentary lithofacies of this area.

Keywords: Petrophysics, Reservoir, Anisotropy, Variogram, Semivariance, Permeability, Alluvial fan, Shale.

Introduction

In exploring for oil and gas, a principal interest is in locating producible reservoir and in other information fundamental to the success of the goal of optimal recovery (Agrawal, *et al.*, 2012; Boyer, *et al.*, 2006; Cipolla, *et al.*, 2011a; Lash, and Engelder, 2011; Goodway, 2001; Marfurt, 2006; Ogiesoba and Eastwood, 2013). These interests are based on the characteristics of the reservoir obtainable from investigations carried out directly or indirectly, that is from either the invasive or non-invasive geophysical means of investigation. Superb vertical resolutions of the temporal well log data makes it attractive for use to interpret and generate results that are indispensable concerning reservoir of interest. Validity of viable hydrocarbon reserve from this temporal data initiates a strong desire to know the possibility of lateral continuity of the interpreted properties away from exploration wells (Marfurt, 2006). This informs the development and use of the seismic method of geophysical exploration for oil and gas. 3D seismic survey is employed to give a clearer picture of what the subsurface rock units are (James, *et al.*, 1994; Biondini *et al.*, 1998), and due to the fact that rocks have elastic properties, the responses of different rock materials to elastic waves is based on density and the velocity of wave travel which constitute the root of seismic theories. Seismic records come with attributes that are intrinsic to the investigated terrain thus there is a desire to know the information shared between wavelet responses and characteristics of rock units (reservoir). An integrated approach to characterizing a reservoir is thus the best in resolving the natural and formative properties of a reservoir (Journel, 1997, 2002; Caers, 2000, 2002; Strebelle, 2000, 2002). The paucity of data and the delicate nature of the few at hand coupled with the very important need to come out with a valid and unassuming exploration philosophy for a particular terrain has informed the need to adequately look inward and properly take into consideration all the properties of the data point available and judiciously incorporate one into another. Models that are valid and peculiar to prevalent geology and depositional environment often result from an interpretation carefully done from a robust database spanning outcrop, seismic, core, well logs, well test and production data. This obviously would have taken into consideration the provenance and current properties of the analyzed rock body. Anisotropy analysis requires evaluating and understanding rock properties based on intrinsic geometrical qualities. These intrinsic qualities are those physico-chemical parameters that have been geophysically measured by various geophysical investigation techniques (Ye, 2010). Physico-chemical parameters (petrophysical properties) vary from point to point in response to the formative conditions and post-depositional changes. Identifying the prevalent variation with direction of deposition is the main interest of anisotropy analysis. An optimum approach for this will be to have a three dimensional view of it for analytical and result plausibility. Hence evaluation in major, minor (horizontal/lateral) and vertical direction becomes indispensable for a robust result.

The Tertiary synsedimentary formations in the Liaohé depression are Kongdian (Ek), Shahejie (Es) and Dongying (Ed) (Hao *et al.*, 2009) (Figure 1). They are paralic, siliciclastic and fluvial-lacustrine generated rock types deposited in restricted environments. Shahejie formation is further divided into four members with their paleoclimate ranging from arid hot northern subtropical to a milder west northern

subtropical climate. They essentially consist of sandstone as reservoir rocks and lithified mud as potential source rocks. There is a remarkable absence of massive reservoir units in the Liaohe depression because of the environment of deposition. Gravity driven mass movement of sediment downhill with little time and space for sediment sorting and consolidation is probably the cause of the heterogeneity and consequently low permeability recorded for the area especially the distal inclined cascading end. The main effect of heterogeneity is often observed on permeability. Presence of fine particle size sediments causes reduction in permeability, blocks tortuosity path and affects oil recovery.

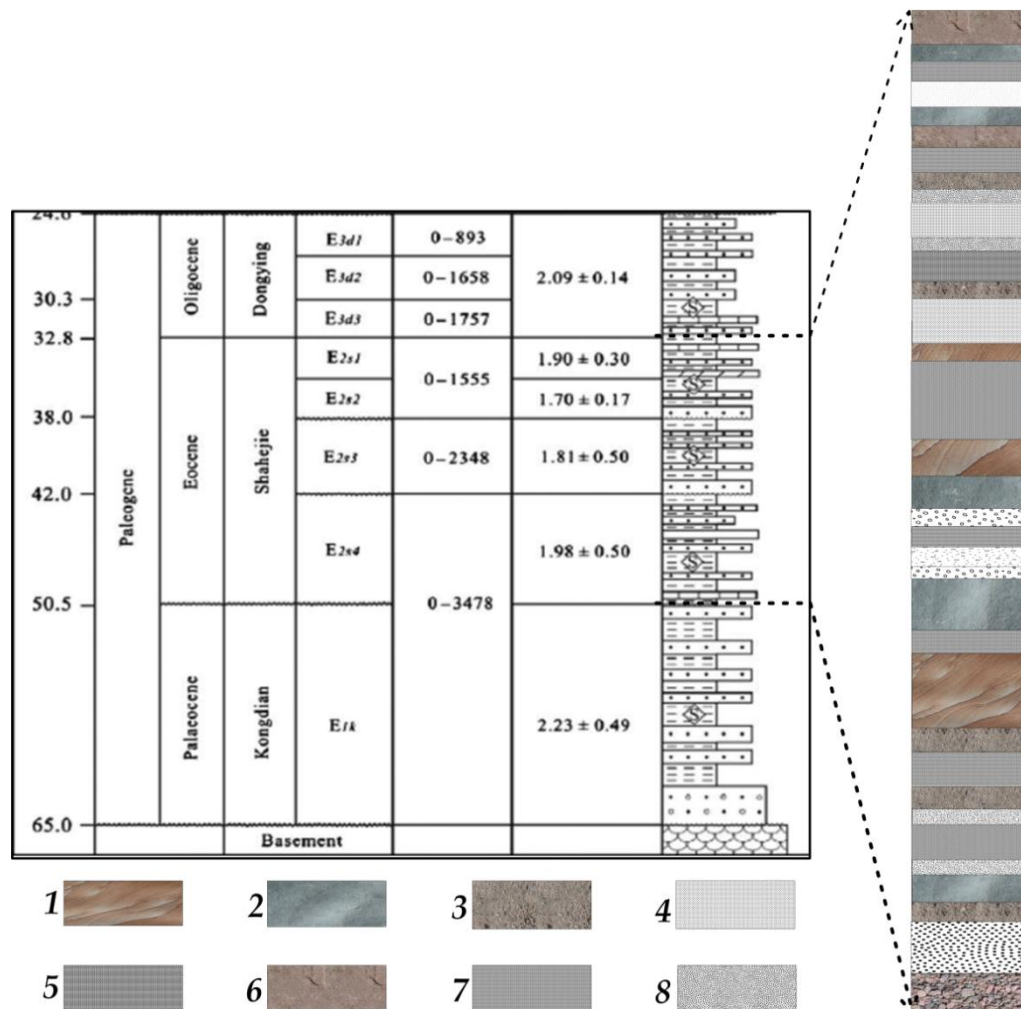


Figure 1: Stratigraphic column of the Tertiary synsedimentary formation of the study area with emphasis on the lithological units of the Eocene Shahejie formation. 1 is cross-bedded Sandstone, 2 is mudstone, 3 is friable sand, 4 is medium grained well sorted sand, 5 is dolomite, 6 is indurated sandstone, 7 is shale and 8 is graded sandstone. (modified from Yinhuiet al., 2011)

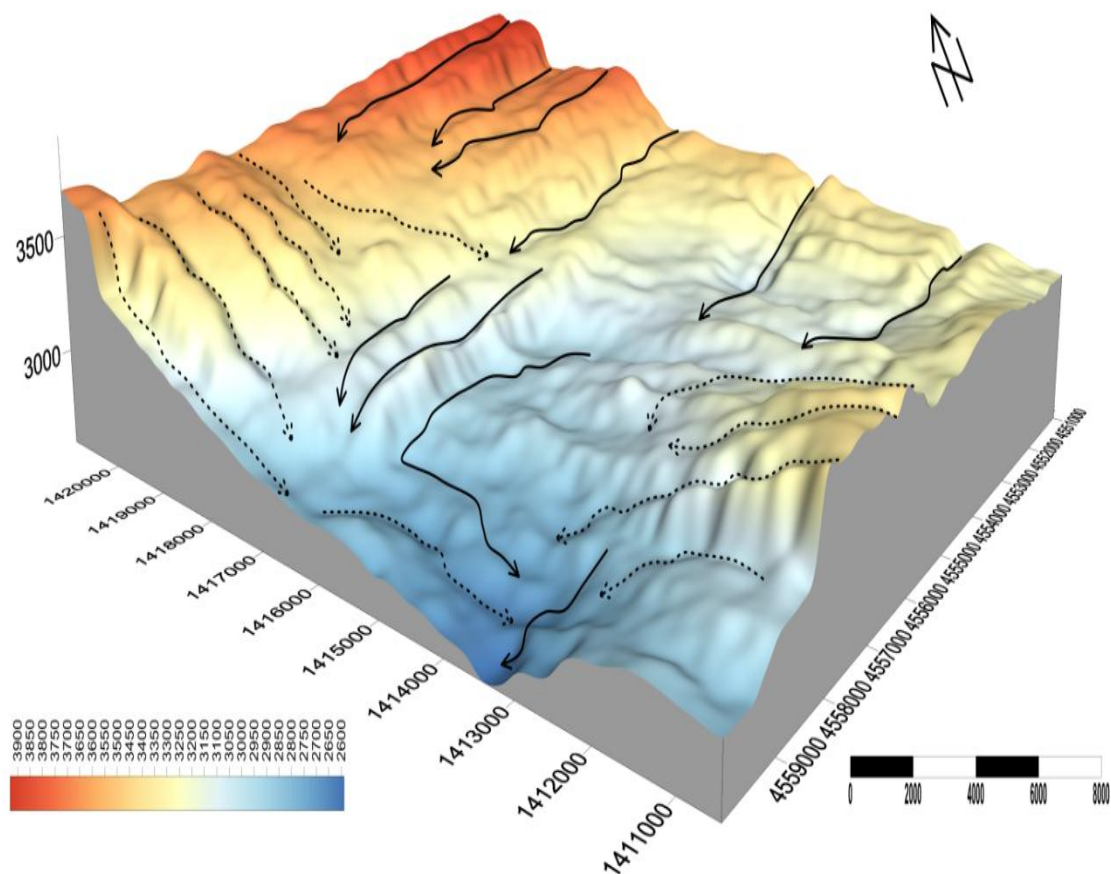


Figure 2: A hypothetical representation of sag structure with path of fluid and sediment motion. This occurs as Alluvial fan environment on the continent while its equivalent is the submarine canyons of the deep sea environment.

The third member of the Shahejie formation (E_{s3}) consist of highly prolific source bed having little terrigenous organic matter and Total Organic Carbon (TOC) content as high as 9.19%, Rock-Eval S_2 values of up to 63.08 mg HC/g rock. Hydrogen index of this member is up to 1115 mg/g TOC signifying remarkable variation in organic matter types (Hao *et al.*, 2009; Gartrellet *et al.*, 2003). Expelled oil from within is injected onto adjacent carrier reservoir bed within the same member and sealed by other adjoining or overlying argillaceous units with competent sealing integrity. Structurally induced instability of the area has cause leaking of oil through fault planes (Gartrellet *et al.*, 2003, 2006; Rotimi *et al.*, 2014). Organic degradation of oil occurs within the reservoir thereby reducing rate of loss of oil while more oil is being expelled onto the carrier beds. This has the tendency to affect petrophysical properties towards recovery. It confers heterogeneity and results in anisotropy of properties all around the oil zone. Understanding the geometrical variation (anisotropy) of rock properties is the main concern of this study.

Geology of Study Area

In Liaohe oilfield, oil and gas exploration began in 1955. The oil flow from well Xin 1 in Liaohe basin revealed the oilfield on 9th September, 1969. As a result of exploration over more than 30 years, 36 oilfields in various sizes have been found with 19×10^8 tonne proven original-oil-in-place (OOIP) and 670×10^8 m³ original-gas-in-place (OGIP). There have been 26 oilfields built up and developed and 9 production bases established, including *Xinglongtai*, Suguang, Huanxiling, Jinzhou, Gaosheng, Shenyang, Ciyutuo, Lengjia and Kerbqin. Now, Liaohe oilfield has established an annual oil production capacity of 1500×10^4 tonne (OilChina Company Limited). Within the Liaohe depression is the study area Xinglongtai-majuanzi structure located in the middle of western sag. The area approaches to panshan sag in the west, Chenjia sag in the north, Qingshui sag in the south, and Lengdong sag, which promote the formation of oil reservoir (Figure 2). Generally, there are six recognized formations reserving hydrocarbon, they include; Archean group, Mesozoic group, Shahejie group and Dongying group of Lower Tertiary of Cenozoic, Guantao Group of Neogene system, Pingyuan group of Quaternary system. It is known that proved geological reserves are 8239×10^4 tonne, and the oil-bearing area is 4.9km². Characteristics of major stratigraphical successions on the field and in the region are also diverse with remarkable variation all across the sub-basins and from the shoreface to the depocentre (Gong, 1997; Wu *et al.*, 2003).

Methodology

Sand tops and horizon interpretation workflow:

Suites of well logs from 6 exploration wells and SEG Y 3D post-stack seismic data obtained from Bohai bay, Northeastern China (Figures 3 and 4) were used. Basic log analysis with emphasis on computations for porosity, saturation, permeability and impedances (acoustic and elastic) initiated well logs interpretation as shown in figure 5. Corrections were applied with the use of standard logs interpretation chart (Schlumberger 2009). This ensures that errors associated with raw logs are filtered off technically, thereby leaving plausible values representing true formation properties. Hydrocarbon cut-off determination was done based on solving equation 1.

$$R_t = \frac{aR_w}{\phi_t^m(1-S_{hc})^n} \quad (1)$$

Where R_t is the resistivity log value, R_w is the interstitial or mud-filtrate resistivity, a is Archie's factor, m is porosity exponent and n is the saturation exponent.

This requires Neutron-Density crossplot, Resistivity log and Archie's exponents amongst other log types. Hydrocarbon reservoir formation (sand tops) identification was based on log signatures and petrophysical properties. Lateral identification of sand tops was done on the seismic workflow through the identification of the respective reflection pattern that characterizes the earlier picked sand tops from well logs. These sand tops were tied to seismic data and 2 horizons S_2 and S_3 were interpreted.

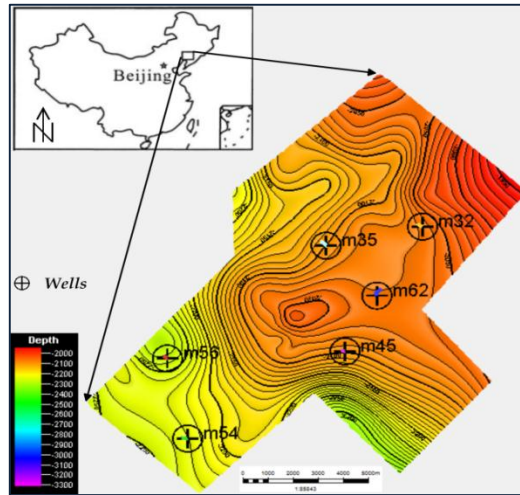


Figure 3: Location of study area

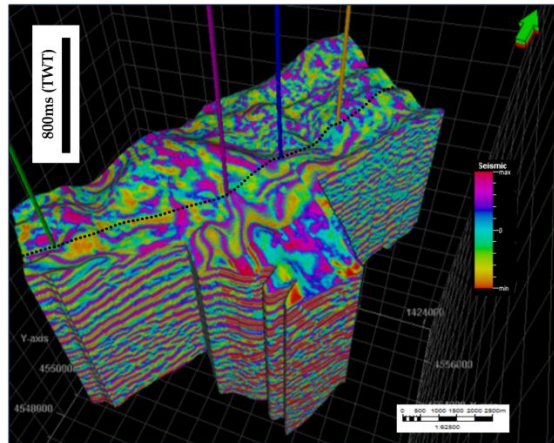


Figure 4: Seismic volume with wells and correlation line as continuous black dotted line

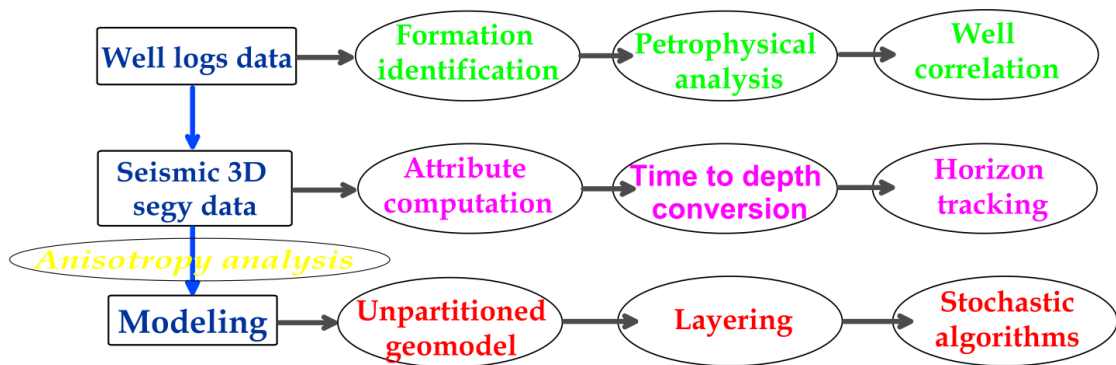


Figure 5: Methodology flow chart

Tracing these sand top formations laterally on seismic data helped in generating the respective horizons (S_2 and S_3) that appeared fairly continuous in reflection amplitudes (Figure 6). They are marked as positive polarity events symmetrical about the wavelet samples. Depth converting the horizons using check-shot data via velocity modeling result allowed its use as casing boundaries for modeling. Computed seismic signal based attribute resulted in clearer reflectors as they are truncated by faulted regions (Ogiesoba and Eastwood, 2013). Structural spatial smoothing was done based on the application of gaussian weighted filter. Dip guiding (i.e. cliff edge enhancement) option was allowed in this process to accentuate the occurrence of dipping beds and preserve them by marking discontinuities. The gaussian filter applied operates as two half filters; an initial step of computing chaos attribute is done to extract variations in amplitude strength continuity. The filter is then applied to the one of the half segment with the highest semblance (lowest chaos) (Figures 7, 8 and 9). Hence edges of discontinuous amplitudes are enhanced. Consequently, contrast in amplitude wavelet became a basis for laterally tracking horizons and eventually defining the containment for simulation operations. Base horizon slope correction for structural attitude continuity within the prograding structurally complex alluvial fan environment made layering an easy step. Geological elements modeling employed the use of formation thicknesses (true/vertical) in defining grid cell designation. Layering followed the response of seismic reflection pattern and basement architecture that influenced the subsurface lithological variations (continuity or truncations). This is due to smoothness or ruggedness, stratigraphically or structurally induced. Similar variations observed on log data are traced both lateral and vertical and was subject to 1D and 2D transformation prior to autocorrelation computation through variogram analysis. Sequential indicator simulation was used for facies modeling to populate the earlier non-partitioned casing built for the zone of interest. The continuous logs upscaled into the simulation case were used as input into the sequential gaussian simulation algorithms. This made possible multiple equiprobable realization of the property volume as randomly generated seed number was used for the modeling operation.

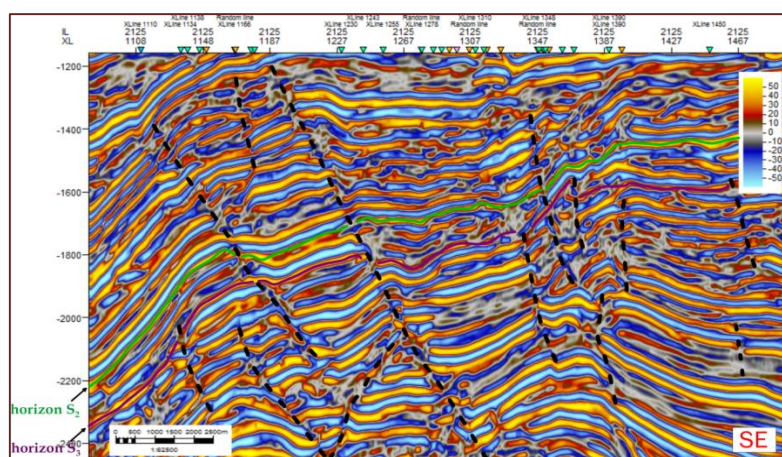


Figure 6: Faults and horizon interpreted seismic line 2125

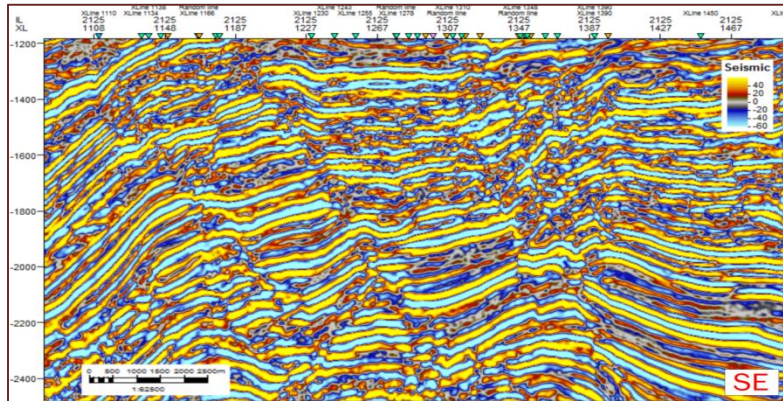


Figure 7: Original amplitude seismic data (line 2125) before applying structural processing via Petrel attribute library

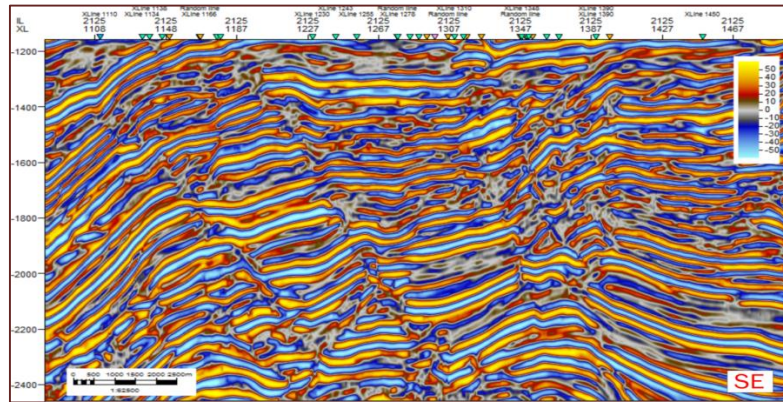


Figure 8: Same seismic line 2125 as in figure 7 after dip guiding edge enhancing structural attribute computation. Faults are seen and defined clearly on this result line.

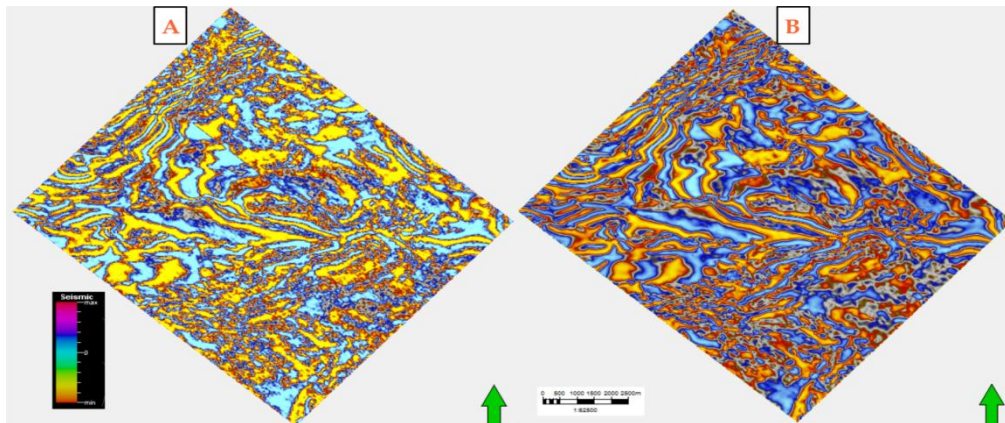


Figure 9: Time slice (A) from figure 7 and (B) from figure 8. Clearer depositional pattern is observed on (B) than (A)

Anisotropy analysis:

Preservation of subsurface structural and stratigraphic features is an intrinsic property of rock deposits. The orientation of both small and large scale features is important for adequate characterization of rock properties. Therefore property variation indices are indispensable in achieving this. Semi-variance plots of all possible data azimuths were plotted on a Cartesian plane. This result in a horizontal variogram map used to define directions of anisotropy. Major and minor directions were inferred from generated maps by observing the contour indicated variance values. The orientation of the direction becomes an input in making sample variogram used in stochastic models of properties. This step was done for all well log data and as a pre-modeling step after well log upscaling. The maximum range used was 30 and search distance was limited to 12,000 m in the x-direction. Half of the distance of x-direction was adopted for the y-direction search distance. The algorithm followed a maximum of 5 cell layers and a standard transformation was done on the hard data.

Results and Discussion**Anisotropy results and variogram maps:**

To find the axis of anisotropy, the use of variogram map is employed (Figures 10-12). This was done for each well logs in the vertical (depth) domain based on each rock properties of interest. This is important for layering operation and for vertically populating the simulation case. Sequel to layering operation, variogram maps were generated and used to determine anisotropy directions (major and minor direction in variation of rock properties). The direction where there is sufficient data to make a stable sample variogram (this is a plot of separation distance of a property against semi-variance of the data) of the modeled property becomes the major direction and the other direction becomes the minor direction. Essentially these directions (major, minor and vertical) are perpendicular to each other; their use, computation parameters and importance are different and independent in application although used together in modeling operations (Deutsch and Journel, 1998; Isaaks and Srivastava, 1989). Variation in sample variogram elements (sill, nugget and range) is what confirms geometrical anisotropy that validates the formative intrinsic geological phenomena. For this study, figures 13-15 are samples of the various anisotropy analyses done for the directions considered. Correlation search cones are seen on the left hand side of figures, sample variogram replica is seen on the right side while variogram parameters are seen above both.

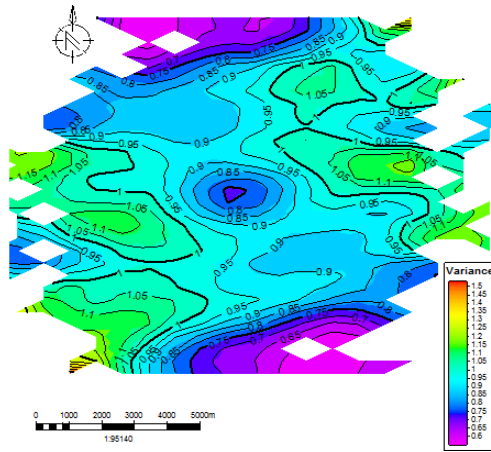


Figure 10: A typical variogram map for porosity data

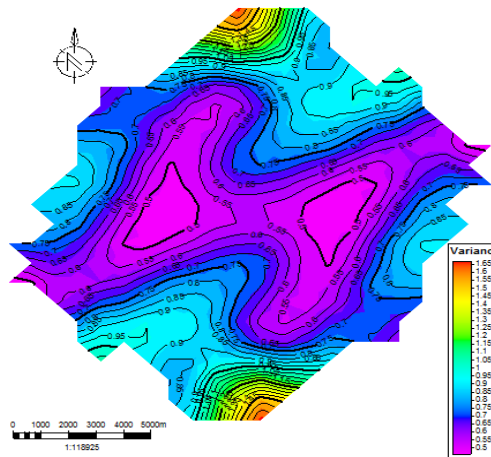


Figure 11: A typical variogram map for permeability data

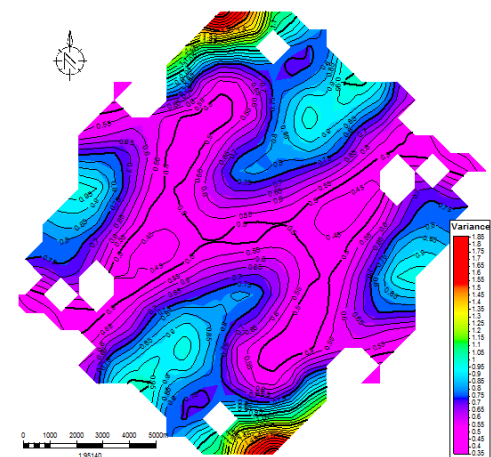


Figure 12: A typical variogram map for volume of shale data

Experimental variograms were computed before making the final variogram function on the autocorrelation spatial dependency for properties analyzed. Results from variogram data analysis gave different directions for the discrete and continuous log data. More variation was observed in the various properties modeled because the major direction was different for all rock properties. This also reflected in the autocorrelation process computed from the variogram analysis. The spherical variogram (Figure 16) and the variations observed on the petrophysical models for the zone of interest seem appropriate for the depositional environment. This is observed on the result of surfaces rendered to know variations in properties with lithofacies models. The middle Shahejie deposits are actually heterogeneous continuous lithological units; they are fairly consolidated lithofacies having intervals of sandy and shaly sequences within a hydrocarbon prolific zone that is probably structurally active (Figure 16).

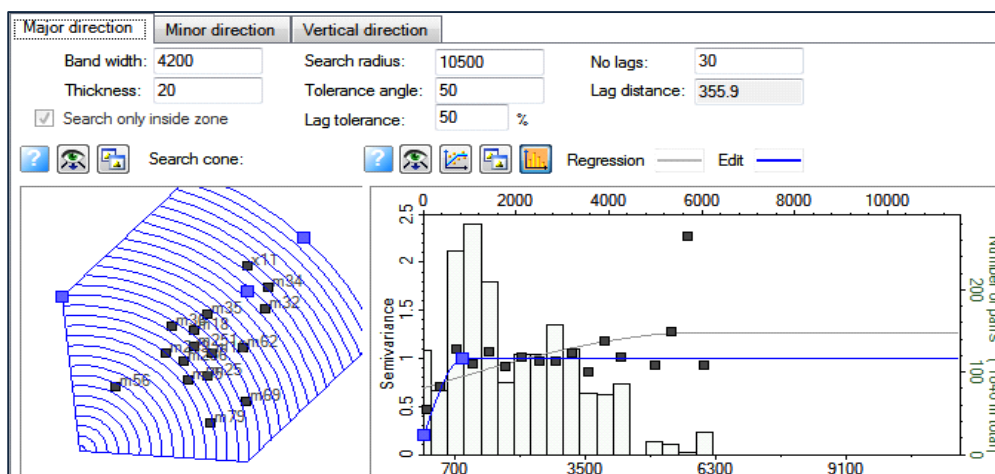


Figure 13: Data analysis panel for major direction

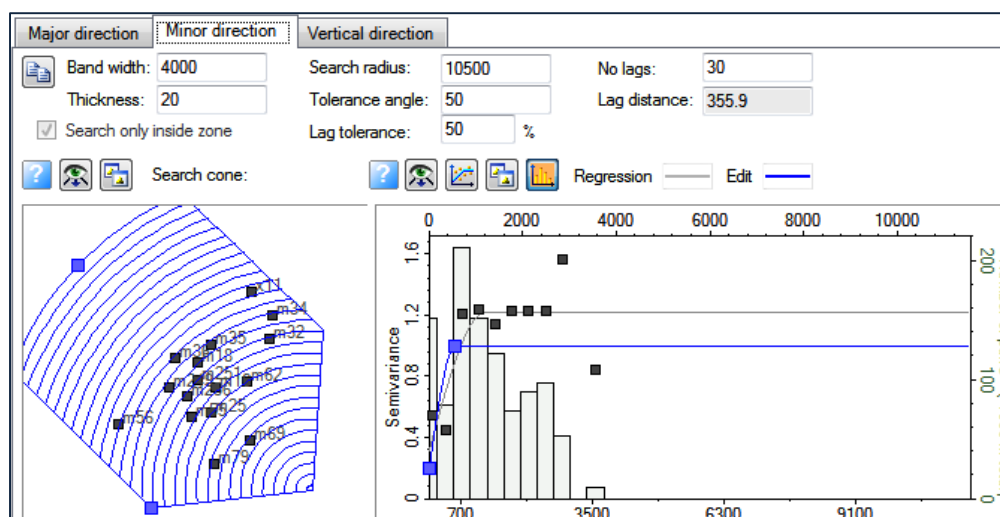


Figure 14: Data analysis panel for minor direction

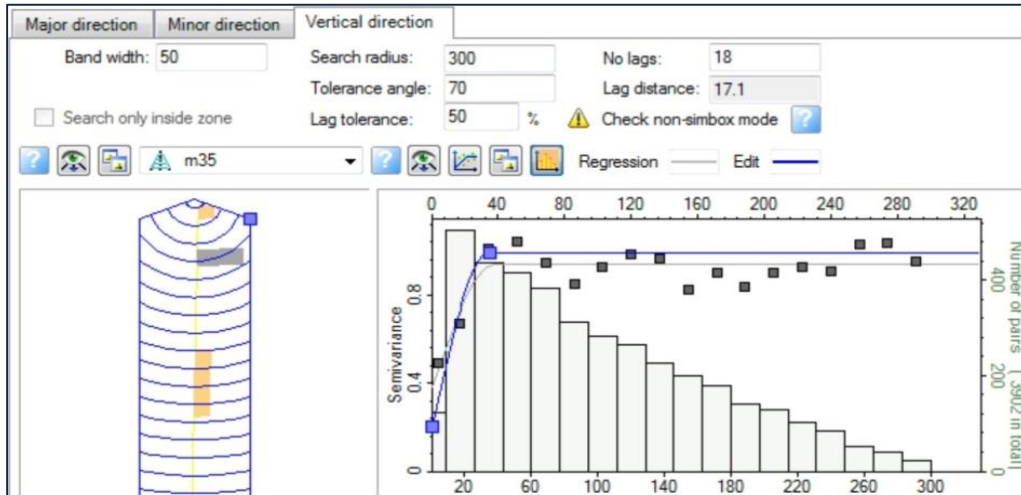


Figure 15: Data analysis panel for vertical direction

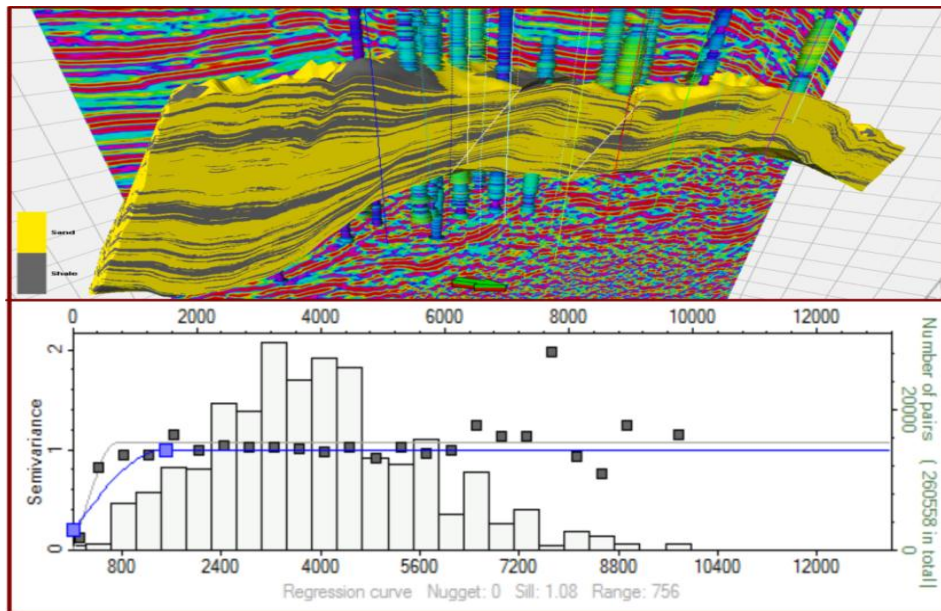


Figure 16: Above-Heterogeneous and continuous nature of the middle Shahejie formation from a combination of facies simulation well logs and seismic data. Below-Experimental variogram computed for the data analysis to observe semivariance all-round the study area.

The anisotropic analysis made it possible to infer continuity and heterogeneity of rock units on hard data (well logs) from rock properties. Evaluating variation of log properties from one location to another vertically and laterally by transforms and auto-correlation coefficients made this possible. This was restricted to the vicinity of oil zone having promising petrophysical properties. The bandwidths and range values

chosen for variogram modeling accounted for the semi-variance between lateral locations of properties. Variogram maps showed northeast-southwest (NE-SW) major direction and minor direction perpendicular to it. This shows semivariance of rock properties located on wells at different levels, thus value dissimilarity on adjacent wells well handled. It resulted into models that have connectivity in properties seen on adjacent wells. Cells designation before and after simulation did well in predicting locations for replicated values as the algorithm progresses successfully to populate the case. Properties projected on intersection/correlation sections on Figure 17 established occurrences of both facies and rock properties at various locations beyond their primary domain as influenced by the various simulation and modeling parameters adopted.

Structural pattern interpretation:

Normal and reverse faults truncates the continuity of rock units on all rock properties modeled on both sides of the fault blocks which form as fault echelons (Figure 18) all round the Northeast-Southwest portion of the field. Some faults were delineated based on subtle reflection discontinuity, marked vertical displacement of adjacent reflection bands shown by abrupt terminations and some by reflection event pattern change across faults (Figure 18). The latter characterized the dipping portion of the area. With the well to well proximity (well offset distance) limited to 300 m taken into consideration, the possibility of estimating occurrences of lithofacies and rock properties was adequately achieved with success both for the inter-well position and also in predicting beyond well location.

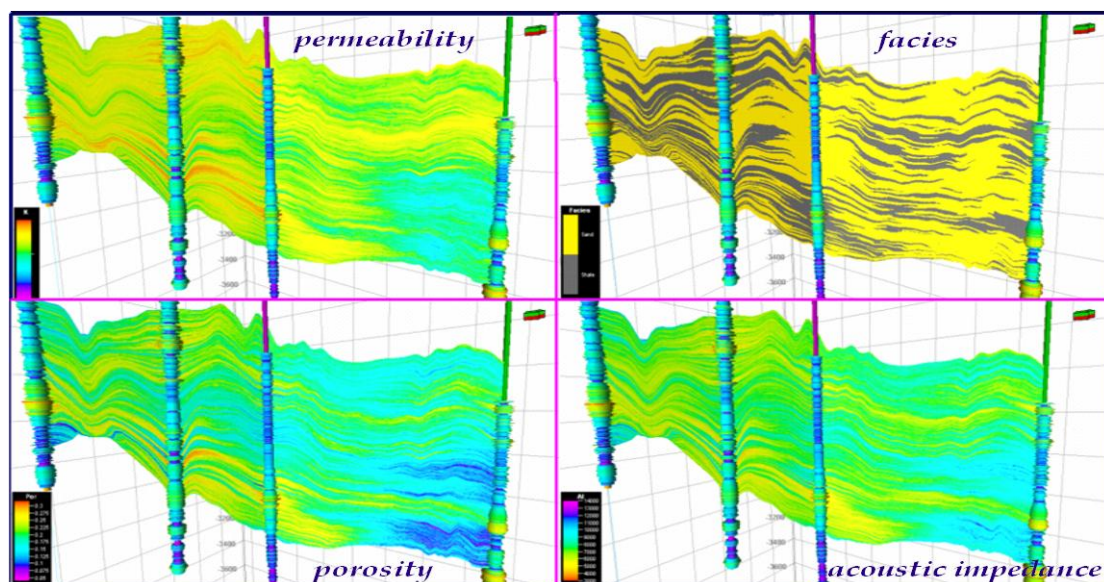


Figure 17: Occurrence of facies and rock properties on intersection plane from correlation line

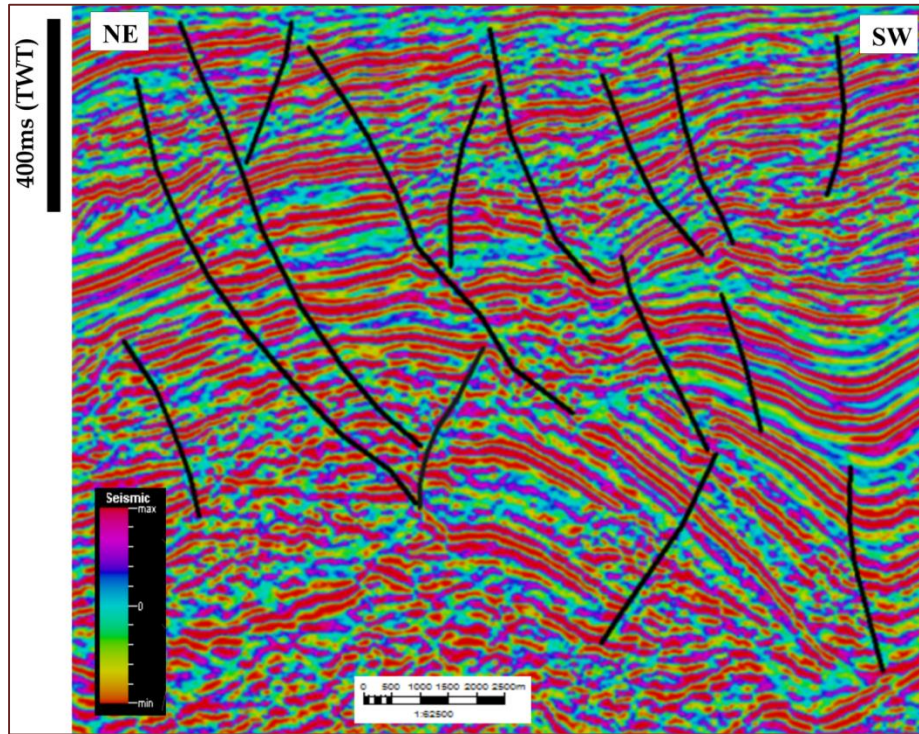


Figure 18: Arbitrary omni-directional fault arrangements characteristic of the area

Lithofacies of this hydrocarbon saturated zone are dipping beds characterized by parallel dipping to sigmoidal reflection patterns on seismic data (Figure 18). Seismic intersection projection of a correlation line shows discontinuous lithofacies on the up-dip portion but a bit continuous in the upper part of the middle portion around wells 62 and 45 (Figure 17). The mixed lithology and rumpled nature of the rock units is observed first on the variations in polarity changing reflection events and amplitude contrast. This is the prevalent pattern amidst the bumpy structural basement architecture mapped on the area (Figure 19).

Lithofacies continuity is rather brief in locations predicted between wells m45 and m54. Sand-shale continuity is obvious between wells m32 and m62. High and low amplitude reflections seen amidst V_{sh} values confirm the randomness of the Shahejie parallel turbidite deposit and the unconsolidated nature of this hydrocarbon bearing zone. The percentage of shale in the section varies laterally across the zone from one well to another. Half of the section (western portion) has shale value on the average between 30% and 50% forming a more homogeneous mix with the reservoir units. The reservoir sand observed below 2400 m on and around well m54 occurs as disseminated bodies. This pithy geobodies appear massive and encapsulated on the facies cross-section around and particularly between wells m45 and m54 (Figures 17 and 19).

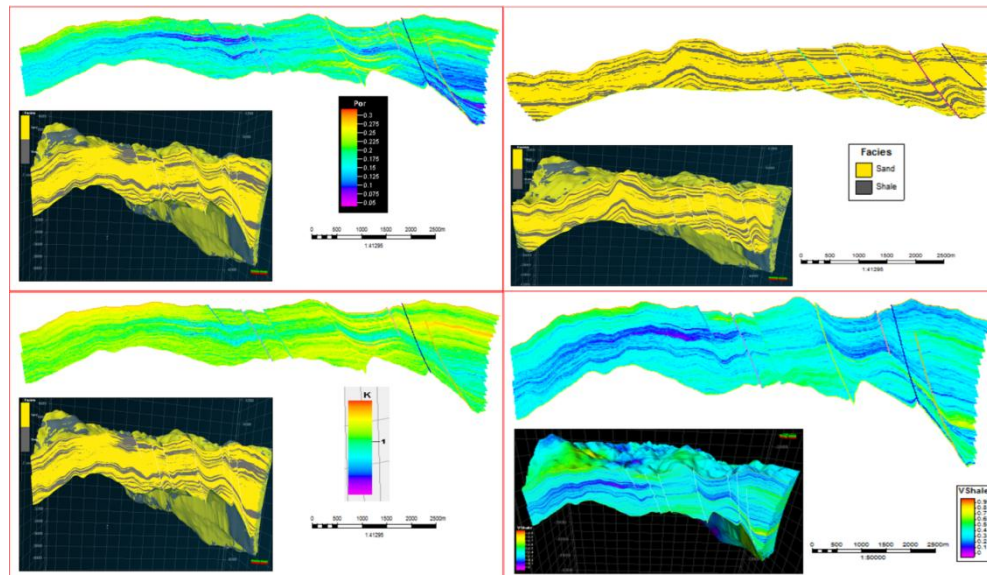


Figure 19: Variation in rock properties against faults. Continuity of properties is seen on both sides of the fault planes

Stratigraphy pattern and lateral continuity on cross-sections:

On well logs correlation panel, stratigraphic patterns range from progradational to retrogradational with most aggradational patterns consisting of mixed interbedded highly porous but fairly permeability shale and silty sand units (Figure 20). Permeable shale is prolific in the area; this is probably because of the poorly consolidated nature of the deposits (Figure 21 and 22). Some units on well logs exhibit blocky pattern with serrated edges. Other fairly diagnostic signatures amidst brief coarsening upward and fining upward lithofacies sequences occurs between some depths (2370m – 2480 m on well m32; 2670 m – 2840 m on well m62) as seen on figure 20. These units appear as fairly continuous reflection patterns on vintage seismic data characterized by inconsistent abrupt terminations. These terminations occur against fault planes that numerous separates trending reflections (Figure 19). Stacks of trending reflection patterns experiences pull down by gravity drag on the dipping distal portion. Characterizing this was basically from trace wavelet polarity reversal and attenuation of amplitude strength. Lithofacies representation for this is clearly shown on cross sections produced from facies model (Figure 23). The wells studied were overlaid on the section with volume of shale as the intersection log property.

In the vicinity of the wells along a correlation line, assessing hydrocarbon saturation against porosity and permeability of rock units shows porous and permeable lithofacies stacks dipping at about 35° Southeast about well m32 (Figure 23). The volume of shale associated with the reservoir rocks of interest reduced down dip towards the toe of the depression. Fluid flow down slope is inevitable in this situation. The likelihood of fluid retention or trapping may be hampered by the altitude and obviously influenced by prevalent structures. This makes porosity and permeability

vary with level of occurrence of different rock types and towards the edge possess spurious values. This validates the effect of geometrical anisotropy analysis done on well log data including petrophysical property logs.

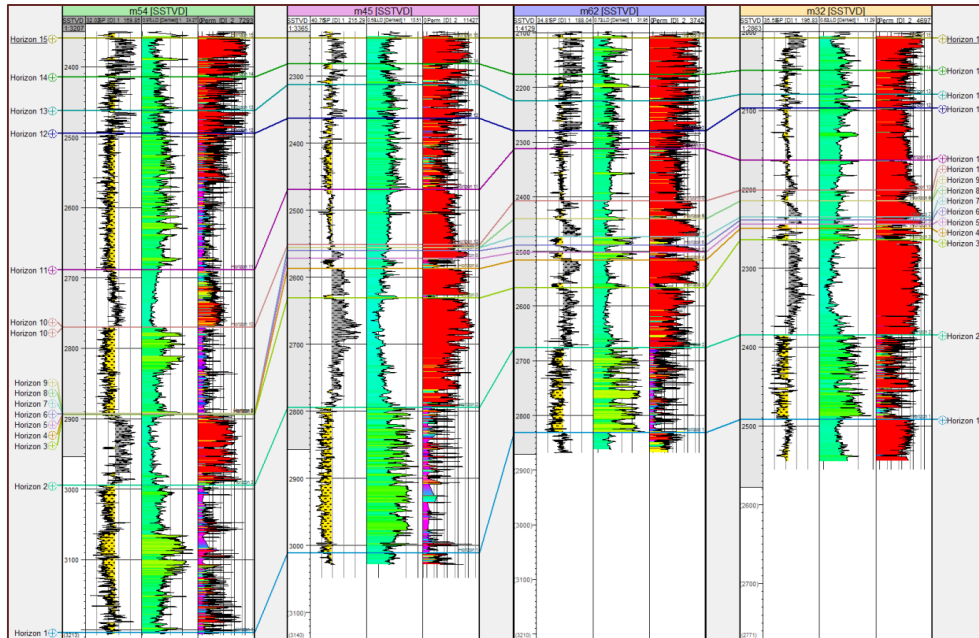


Figure 20: Correlation panel for 4 wells. Sand and shale sequences are seen. The shale units are seen to be quite permeable but impregnated oil not producible with natural drive. Permeability is on track 3. See figure 4 for location of correlation line

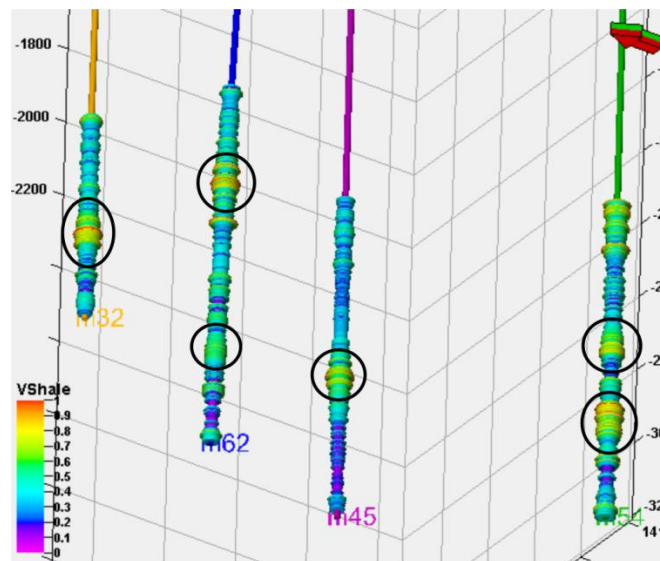


Figure 21: Section of well logs showing portions with high value of shale

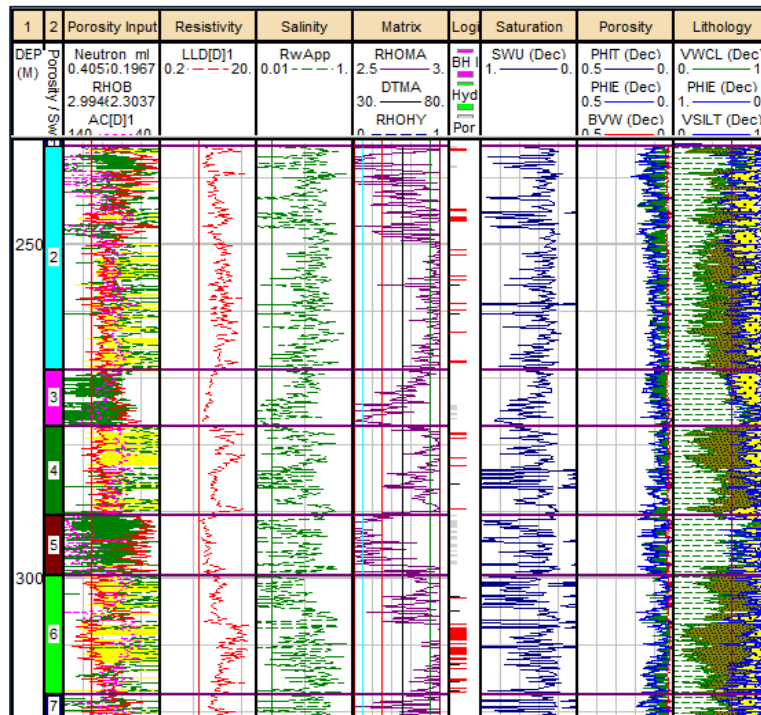


Figure 22: Petrophysical interpretation panel for well m32. Note the lithology mix of silty sand and shale in the last track (lithology)

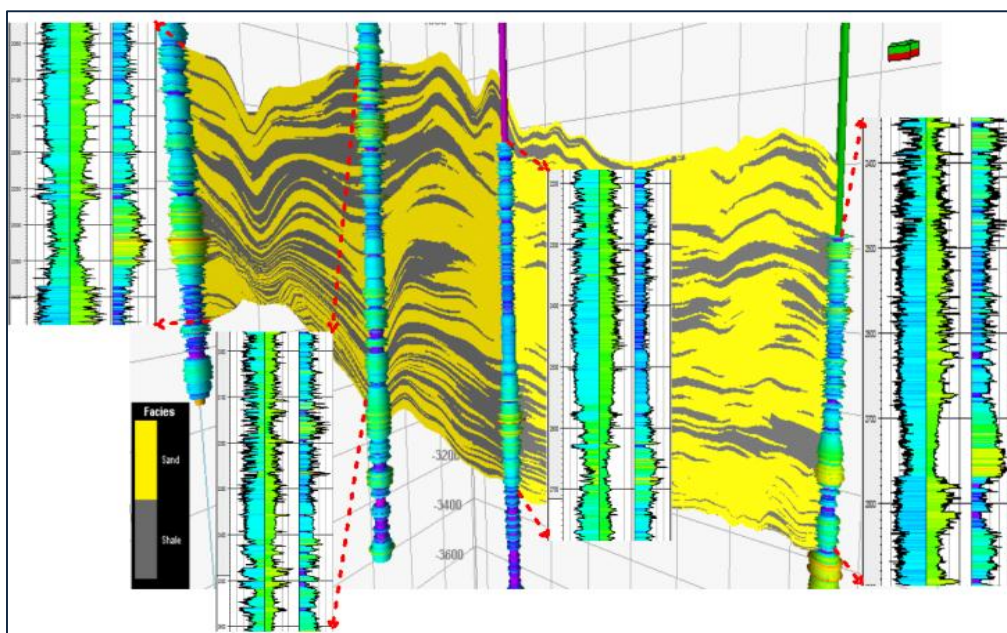


Figure 23: Petrophysical interpretation panel for well m32. Note the lithology mix of silty sand and shale in the last track (lithology)

Reservoir rock fluid properties:

Sandstone reservoir units traced laterally range in thickness between 0.3m and about 130m. On all wells, there are condensed sand unit in the middle and towards the base (between 2378 m and 2490 m on well m32). Above it is a thick non-hydrocarbon bearing formation, and towards the top are other reservoir units of smaller thicknesses. The reservoir sand unit between 2248 m and 2268 m has average porosity value of 0.15. All reservoir sand units in the lower, middle and upper portions of the well extend laterally to the next well 45. This lateral continuity grades into interfingering of brief and thin sand and shale sequences with varying depths. Their porosity is between 0.14 and 0.25 (Figures 17, 19, 20, 21, 22 and 23). A different lithofacies arrangement is observed on the most distal well m54. The middle portion has massive reservoir unit with fewer intermittent occurrence of shale formations. This region is observed to be the most hydrocarbon prolific with porosity of above 0.18 and permeability of more than 4mD. The lithofacies pattern on well 62 is more of graded sand and shale units. This well is in the proximal end of the block, the reservoir sand unit occurs in massive deposit of about 60 m between 2810 m and 2870 m. Other portions are also consistent with average porosity of 0.14 and appreciable hydrocarbon saturation (Figures 17, 19 and 22). Common porosity value for these sandstone units is in the range 0.1 to 0.25; the permeability observed is between 1 and 2.2mD. The volume of shale values is between the range of 0.2 and 0.4 for the sand zones.

A collective assessment of properties and potentials of the zone for hydrocarbon accumulation is seen on a group of some subsurface maps produced from seismic attribute computations and results of rock property model simulations (figure 24). Root mean square (RMS) amplitude, instantaneous amplitude (reflection strength) both show gathers of reflection intensity in the vicinity of wells studied. Seismic attribute maps generated shows realistic variation of rock properties from the analysis of the subsurface reflection events. Other maps show distribution of porosity and permeability. This two rock property has given a good match with the lithofacies distribution on the area with well. Patterns indexed by peak amplitude values on maps are clearly mimicked by the concentration of porosity in like manner around well points in response to geometrical anisotropy analysis. Lateral variation on permeability map follow a fairly uniform lithofacies distribution pattern within the stratigraphic attitude. This complements the porosity and seismic attribute map patterns (Figure 24).

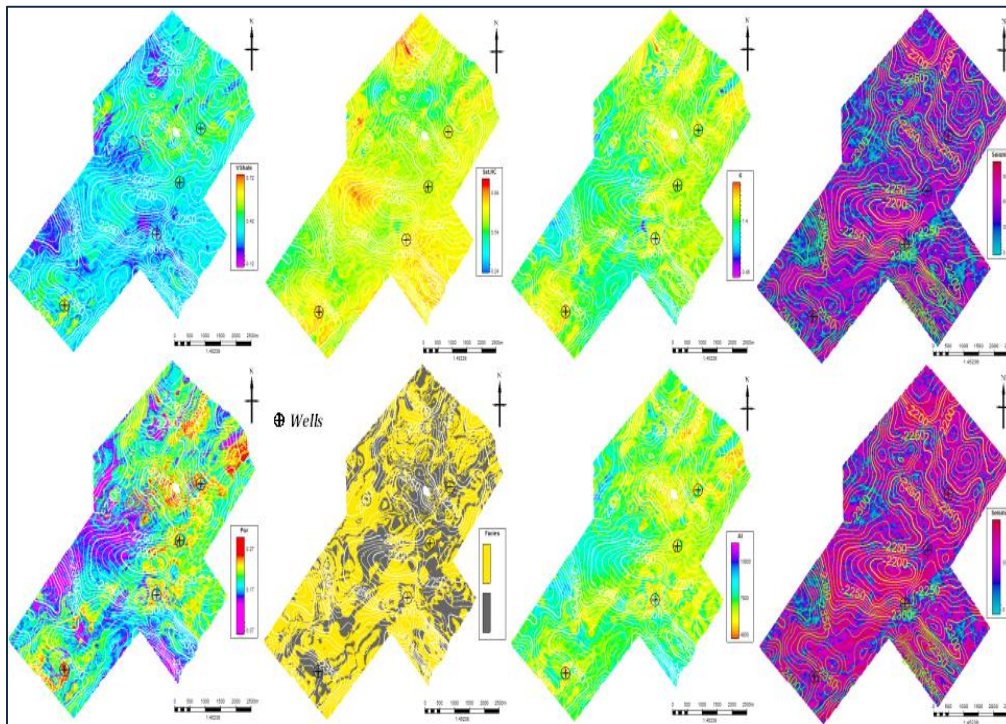


Figure 24: Maps of rock and fluid properties for the area. This captures between horizons S_2 and S_3 . Lateral variations in properties are seen in locations around and beyond well points

Acoustic impedance simulated surface shown in figures 17 and 24 adequately characterized the lithofacies distribution shown in the facies model surface. This clearly defines the units designated sand as porous and also indicating same as having adequate permeability both laterally and vertically.

Conclusion

Geometrical anisotropy analysis has been considered in understanding prevalent variation in petrophysical and rock properties using well logs and seismic data. This entails computation of both horizontal and vertical autocorrelation coefficient as main input in modeling operations. Different stochastic algorithms and property collocation modeling with the a priori based on the autocorrelation tendencies of the pre-simulated rock properties has been done. Geometric prediction done resulted in both interpolation and extrapolation of rock properties as an estimate that was initiated from temporal log data upscaled and allowed to be distributed stochastically. The non-simbox modeling approach is appropriate for characterizing deposits in terrains with similar geology and depositional environment. Observed variations are essentially stratigraphy induced but structurally controlled. It has application in reserve evaluation when properly done and adequately integrated with production data

to examine and determine hydrocarbon and recovery potential for unconventional reserves. It is also a good method for defining stratigraphic continuity and tracing the distribution of rock properties within an area of interest.

Acknowledgement

TWAS-CAS is appreciated for study fellowship granted for this work, we also thank IGGCAS and Covenant University for their support in the course of this study. Liaohe oil field is appreciated for the release of data and permission to publish. The China Ministry of Science and Technology is appreciated for the equipment donation made available for this research under the CASTEP scheme.

References

- [1] Agrawal, A., Wei, Y., and Holditch, S. A., 2012. A technical and economic study of completion techniques in five emerging US gas shales: A Woodford Shale example. SPE, 27, 39-49. doi: 10.2118/135396
- [2] Biondi, B., Mavko, G., Mukerji, T., Rickett, J., Lumley, D., Deutsch, C., Gunderso, R. and Thiele, M., 1998. Reservoir Monitoring: A Multidisciplinary feasibility study: *The Leading Edge*, 17, pp 1404-1414.
- [3] Boyer, C., Kieschnick, J., Suarez-Rivera, R., Lewis, R. E., and Waters, G., 2006. Producing gas from its source: Oilfield review/ Schlumberger, 36-49.
- [4] Caers, J., 2000. Modeling facies distributions from seismic using neural nets, Stanford Center for Reservoir Forecasting Annual Report, 1(13), 1-30
- [5] Caers, J., 2002. History matching under training-image based geological model constraints, Stanford Center for Reservoir Forecasting Annual Report, 1(15), 1-19
- [6] Cipolla, C., Lewis, R., Maxwell, S., and Mack, M., 2011a. Appraising unconventional resource plays: Separating reservoir quality from completion effectiveness: International Petroleum Technology Conference, Paper IPTC 14677.
- [7] Clayton V. Deutsch, Andre G. Journel 1998. GSLIB Geostatistical Software Library and User's Guide, Second Edition.
- [8] Edward H. Isaaks, R. Mohan Srivastava 1989. An Introduction to Applied Geostatistics. Oxford University Press, New York, p. 561.
- [9] Goodway, B., 2001. AVO and Lamé constant for rock parameterization and fluid detection. CSEG Recorder, 26(6), 39-60
- [10] Gong Z. S., 1997. Giant offshore oil and gas fields in China, Beijing. *Petroleum Industry press*, pp. 396.
- [11] Hao F., and J. Y. Chen, 1992. The cause and Mechanism of vitrinite reflectance anomalies. *Journal of Petroleum Geology*, 15, 419-434
- [12] Hao F., J. Y. Chen and Y. Z. Liu, 1993. Application of organic facies studies to sedimentary basin analysis-A case study from Yitonggraben, China. *Organic Chemistry*, 20, 27-43

- [13] Hao F., Zhou X., Zhu Y., Bao X., and Yang Y., 2009. Charging of the Neogene Penglai 19-3 field, Bohai Bay Basin, China: Oil accumulation in a young trap in an active fault zone. *AAPG Bulletin*, 93(2), 155-179.
- [14] James, H., Tellez M., Schaetzlein, G., and Stark, J., 1994. Geophysical Interpretation from Bits and Bytes to the Big Picture. *Oil Field Review*, 7, 23–31.
- [15] Journel, A. G., 1997. Deterministic geostatistics: a new visit, in Baffi, E. and Shofield N. eds., *Geostatistics-Wollongong*, 1, Kluwer Academic Press, Dordrecht, pp. 174-187.
- [16] Journel, A. G., 2002. Combining knowledge from diverse information sources: an alternative to Bayesian analysis, *Journal of Mathematical Geology*, pp 639
- [17] Lash, G., and Engelder, T., 2011. Thickness trends and sequence stratigraphy of the middle Devonian Marcellus Formation, Appalachian Basin: Implication for Acadian foreland basin evolution. *AAPG Bulletin*, 95, 61-103, doi: 1306/06301009150
- [18] Marfurt, K. J., 2006. Seismic attribute mapping of structure and stratigraphy: Distinguish instructor short course series, SEG, 268.
- [19] Ogiesoba, O. C., and Eastwood, R., 2013. Seismic attribute analysis for shale gas/oil within the Austin Chalk and Eagle Ford Shale in a submarine volcanic terrain, Maverick Basin, South Texas. *Interpretation*, 1(2), SB61-SB83.
- [20] Rotimi O. J., Ako B. D., Zhenli W., 2014. Application of Rock and Seismic Properties for Prediction of Hydrocarbon Potential. *Journal of Petroleum & Coal* 56 (1), 40-53.
- [21] Strebelle, S., 2000. Sequential simulation drawing structure from training images. Unpublished PhD Thesis, Stanford University, Stanford, CA, USA. 140p
- [22] Strebelle, S., 2002. Conditional simulation of complex geological structures using multiplepoint statistics. *Mathematical Geology*, 34, 1-22.
- [23] Wu, L., H. M., Xu and J. H. Cheng, 2006. Evolution of sedimentary system and analysis of sedimentary source in paleogene of the Bozhong sag, Bohai Bay (in Chinese with English abstract). *Marine Geology and Quaternary Geology*, 26, 81-88.
- [24] Ye, F., 2010. Anisotropy of the Bakken Formation, East Williston Basin, North Dakota: Presented at the UT-Austin Edger Forum
- [25] Yinhuai, Z., Nansheng, Q., Yuan, Z., Cuicui, L., Jianping, L., Yonghua, G., and Xiongqi, P., 2011. Geothermal regime and hydrocarbon kitchen evolution of the offshore Bohai Bay Basin, North China. *AAPG Bulletin*, 95(5), 749–769

